SMiRT-12 / K. Kussmaul (Editor)

E05/3

EVALUATION OF THERMAL RATCHETTING ON AXISYMMETRIC THIN SHELLS AT THE FREE LEVEL OF SODIUM: EXPERIMENTAL RESULTS AND ELASTIC ANALYSIS

M.T. Cabrillat, J.M. Gatt, P. Schoulguine and A. Skiara

CEA Cadarache, 13108 Saint Paul Lez Durance Cedex, France

1 INTRODUCTION

Startup operations and load variations for a FBR reactor (Fast Breeder Reactor) cause sodium level variations in the vessels which exert stresses on the emergent shells in the free level area. The loading of these shells is mainly linked to the axial thermal gradient, primary stresses being generally low or negligible as are the radial thermal gradients.
Under the effect of these variable axial thermal gradients, there is a risk of progressive deformation even in the absence of primary type stresses (reference 1).
The simplified methods of analysis (Bree diagram, efficiency diagram) proposed in the design codes (Code Case and RCCMR) are not applicable in this specific case where primary type stresses are negligible.
In recent years, many studies and experimental programmes have been undertaken in order to propose more reliable methods of analysis for these structures.
This paper describes the experimental program, called VINIL, developed at the CEA at Cadarache. After a brief description of the experimental facility and of the experimental results, this paper proposes an evaluation of the risk of progressive deformation on an elastic basis : various simplified methods of analysis were used and are compared with experimental results.

2 EXPERIMENTAL PROGRAM

2.1 Facility

The purpose of the VINIL tests is to study the problems related to variations of free levels on mock-ups subjected to loading representative of the actual loadings exerted on structures during reactor operation.
The experimental facility must allow the simulation of variations in temperature and level during shutdown and startup operations and in the course of load variations. In addition, we felt it was important to represent hold times at high temperature in order to take into account any interaction between creep and progressive deformation.
A diagram of the experimental facility is provided in figure 1. The test mock-up (cylindrical shell : 800 mm diameter, 1.2 mm thick) is placed in an annular space filled with sodium. An electromagnetic pump running in continuous mode at low output is used to ensure filling of that space. An overflow system maintains a constant sodium level in the space. Level variations are simulated by vertical displacement of the mock-up, this displacement being obtained using a motorizing system.
Finally, the sodium is heated by means of three heating elements of the pyrotenax type.

2.2 Mock-up

Two different mock-ups were used for the tests :

- a mock-up referred to as a "long mock-up" which is embedded on its upper section and which features a length between the position of the free level and the embedded section which is greater than the shell decay length,

- a mock-up referred to as a "short mock-up", which is free on its upper section and which has an emergent height that is smaller than the shell decay length. In addition, four 35 mm slots were made in the upper section in order to limit the stiffness of the emergent area while retaining a sufficient length to obtain significant thermal loading. The minimum emergent resistant height was therefore equal to 20 mm.

As this mock-up was free on its upper section, the attachment method was modified. The mock-up was secured by the bottom to a shell of smaller diameter, referred to as the "bearing shell", which was embedded on its upper section in the same way as the mock-up previously mentioned. We therefore have a double shell in this case.
The two test mock-ups were cylinders with a diameter of 800 mm and a thickness equal to 1.2 mm. They were fabricated using steel plates of type 316 and have two meridian welds. Stiffening ribs in the lower section immersed in sodium allowed the structure to be stiffened. Finally, these mock-ups were annealed in order to eliminate the strain hardening due to their manufacture.
Characterizing tests were performed after annealing. It is observed that the material characteristics are very close to the data for the RCCMR material 1S.
Finally, very extensive thermocouple instrumentation was intalled. About one hundred thermocouples were distributed on the test facility itself and about forty on the mock-up in order to verify the satisfactory operation of the test as well as to obtain accurate measurement of the thermal fields sustained by the mock-up.

2.3 Metrology

It is of prime importance for this type of test to have access to the deformations to which the structure is subjected. This measurement cannot be performed in continuous mode during testing (sodium environment at 620°C). Periodic disassembly is required. A specific measuring bench was made. This allowed the acquisition of 200 points per circumference with an axial pitch of 2 mm in the area of interest.

2.4 Loading

An operating cycle must allow the simulation of the variations in temperature and sodium level occuring during an actual operating cycle on reactor.
The temperature variations are obtained by controlling the heating elements. The temperature of the sodium rises from 200°C at the beginning of a cycle to 620°C. It is held at that temperature for 50 mn and then cooled down to 200°C. The temperature of 620°C was chosen in order to accelerate the effects of creep and to limit the duration of temperature holding times.
In parallel, the test shell must be moved in order to represent the variations in sodium level (see figure 2). When the temperature of the sodium reaches 620°C, the shell is lowered by 35 mm in 15 seconds which simulates an increase in the volume of sodium. This position is maintained throughout the duration of the temperature hold time at 620°C. The cooling of the sodium and the upward movement of the shell (35 mm in 15 seconds) are then triggered simultaneously. A time lag is introduced on return to the cold temperature in order to ensure complete cooling of the whole mock-up.

3 EXPERIMENTAL RESULTS

3.1 Long mock-up

Three successive campaigns were performed using the long mock-up. Disassembly operations were performed for measuring purposes after 500 cycles, 700 cycles and 930 cycles. In addition, an initial measuring operation had been performed before the beginning of the tests.
After 500 cycles, a major deformation was observed in the free level variation area, corresponding to a decrease in radius : the maximum value recorded was equal to $\Delta R = -1.6$ mm, i.e. approximately 1.3 times the thickness, which corresponded to a circumferential deformation of 0.4 %. If the mean value of these deformations is calculated for all the generating lines recorded, a decrease of $\Delta R = -0.8$ mm is obtained (see figures 3 and 4).

It is noted that these deformations are essentially developed in mode 0.
After 700 cycles, we observe an amplification of these mode 0 deformation corresponding to a further decrease in the radius of 0.1 mm, i.e. an additional circumferential deformation of 0.025 %. We therefore note that the variation is much less than during the first campaign.(see figure 5)

Finally, after 930 cycles, it appears that this radial deformation located near the level variation zone stabilizes. No significant change is noted between 700 and 930 cycles. But deformations on higher modes (mainly mode 3) become important.

3.2 Short mock-up

Two short campaigns were carried out on this mock-up, the first consisting of only 12 cycles and the second consisting of 73 cycles (making a total of 85 cycles). The deformations recorded were very different from those obtained on the long mock-up : in particular, no decrease in radius in mode 0 was noted in the vicinity of the free level area but, rather, a deformation in a preponderant mode 4 was observed over a significant length, probably in relation with the presence of the four slots.(see figure 6)
After 85 cycles, the results were similar but amplified.
We thus noted that the limit conditions had a great influence on the deformations obtained during the tests. The long shell was subject to the progressive deformation phenomenon according to a preferential mode 0, localized in the free level variation area.
For the short shell only the deformation corresponding to higher modes exist in relation with limit conditions.

4 INTERPRETATIONS

Interpretative calculations have so far only been performed on the long shell, with the aim of obtaining mode 0 deformations. Initial defects were not considered.
At a first stage, thermal calculations were peformed in order to obtain the variation in thermal fields during the transient. In these calculations, allowance was made for heat exchanges by conduction and by convection with the sodium and argon respectively, temperature variations of the sodium and, also, level variations.
It is verified that extremely good consistency is obtained with the temperatures recorded during the test.
Elastic mechanical calculations were then performed on the basis of those thermal data, using the material data from RCCMR A3-1S.
During a cycle, the axial and circumferential stress vary in the free level variation area. The axial stresses are mainly bending stresses, whereas the membrane is preponderant in the case of circumferential stresses.
The maximum stress variations are obtained on the outer skin of the shell, slightly below the sodium level high position. Figures 7 and 8 show the variation of the axial and circumferential stresses on the outer skin at the two transient instants found to be dimensioning, i.e. 11 seconds and 25 seconds after the start of the variation in level.
The variation in maximum equivalent stress is equal to : $\Delta\sigma VMmax = 342.6$ MPa with, for the two corresponding instants :

T1 : $\sigma z = -48.80$ MPa $\quad\quad \sigma\theta = 77.00$ MPa
T2 : $\sigma z = 165.90$ MPa $\quad\quad \sigma\theta = 103.44$ MPa

These elastic stress results were then used to evaluate the risk of progressive deformation using various existing methods.

4.1 Efficiency diagram, RCCMR 1987 issue

As the primary stresses were null in our case, this method is not applicable.

4.2 Bree diagram

In this method, the primary and secondary stresses calculated elastically are used to evaluate an effective creep stress σc which is then used to determine the total strain, taking the progressive deformation into account.
In the specific case of the VINIL test, as the primary stress was null, the representative point is located on the axis of the secondary stresses in the plastic shakedown domain. In this domain :

$$\sigma c = \frac{P}{Sy} \cdot \frac{\Delta Q}{Sy}$$

Given $P = 0$ therefore $\sigma c = 0$. The method is not applicable.

4.3 Shakedown method, lower bound

This method is not applicable as the whole thickness of the shell is plastified.

4.4 Shakedown method, upper bound (Reference 2)

Specific diagrams were proposed to deal with the case of shells submitted to variable axial thermal gradients. In this case, the authors evaluated the boundary between the plastic shakodown domain and the thermal ratchetting domain in relation to a parameter F which is a measurement of the severity of the variation of the thermal gradient.

The point (C, T) corresponding to the maximum loading of this structure is then positioned on this diagram in order to determine the region in which it is located. C and T are the standardized mechanical and thermal stresses (Tresca), respectively.

Figure 9 shows the application to the VINIL mock-up. It will be noted that the point is in the thermal ratchetting domain.

4.5 Japanese method (References 3 and 4)

The authors proposed a new method for the evaluation of progressive deformation in the specific case of cylinders subjected to temperature distributions that are variable in space. For a first approach, the primary stresses as well as the axial bending stresses were assumed to be negligible. Supplementary studies allowed this method to be improved and led to the proposal of diagrams taking all the stresses into account. It should be noted that these diagrams can be used in the absence of primary stresses.

Finally, the increment of progressive deformation per cycle ϵR is evaluated in the following manner :

$|\epsilon R| = 2\,(|\sigma\theta el| - (\sigma y)/E = Z.\,\sigma y/e$

Where σy is the equivalent yield stress dependant on the stress state

$\sigma y = \sigma y\,(\sigma\theta el, \sigma zel)$

with : $\sigma\theta$: circumferential membrane stress

σz : axial bending stress

The diagram allows to obtain the value of parameter Z on the basis of :

$X = (\sigma\theta el + \sigma p)/\sigma y \qquad Y = \Delta\sigma zel/\sigma y$

Finally, to take into account cyclic strain hardening which tends to cause a decrease in the plastic deformation increment, the final deformation is written as follows :

$\epsilon R = \Sigma hi.Z.\sigma y/E = h.Z.\sigma y/E$

with h tending towards the value 25 for 304 steel.

By applying this method to the VINIL tests on the basis of elastic calculations, we obtain :

$X = 1.43 \qquad Y = 2.20$

Whence : $Z \sim 1.0$ and $|\epsilon R| = 0.076$ %.

If we adopt the same coefficient, h, as for 304 steel, a final deformation equal to 1.90 % is forecast.

It should be noted, however, that the creep effects are not taken into account in th is method and that, consequently, the forecast must be further increased. It thus seems that this method is extremely conservative for this loading case.

4.6 Extension of the efficiency diagram method

The efficiency diagram method described in RCCMR, 1987 issue, does not allow this type of problem to be dealt with. Thanks to recent work, it has been possible to generalize this approach (see reference 5). The main idea consists in considering the mean stress working during the first cycle as primary stress P* for the application of the efficiency diagram.

For the specific case of the elastic analysis in the VINIL test, this amounts to starting with the maximum circumferential membrane stress $\sigma\theta m$ which is redistributed on the material behaviour curve by using an elastic follow up coefficient in order to obtain an estimate of the actual stress σ. The primary stress used for the efficiency diagram application is thus taken to be equal to : $P^* = \sigma/2$.

The value of the elastic follow up coefficient is evaluated in a conservative manner (see reference 6) :

$$r_m = \frac{n-1}{2}$$

By redistributing the maximum circumferential membrane stress $\sigma\theta = 157.3$ MPa on the mean monotonous curve for the material, we obtain : $\sigma = 128$ MPa and $P^* = 64$ MPa.

The efficiency diagram application leads to : Peff = 148 MPa.

The two conditions : Peff < 1.2 Sm and U $(\frac{Peff}{1.2})$ < 1 are not verified.

The design of this structure would therefore, not be admissible with respect to RCCMR.
Furthermore, we can estimate the final strain that is predicted on the structure. On the mean monotonous curve, σ = 148 MPa corresponds to a plastic strain of approximatively 0.42 % and, on the mean isochronous curve corresponding to the test duration (930 cycles with a holding time of 50 mn), it corresponds to a deformation of about 1%.

5 CONCLUSION

The tests carried out on the VINIL mock-ups show that progressive deformation does, in fact, occur but that the deformations obtained greatly depend on the limit conditions (whether the shell is short or long, free or embedded) as well as on the initial geometry.
For the long shell, which is used to test the various methods of analysis, we obtain a stabilization of the deformations after 700 cycles. The residual maximum circumferential strain obtained is about 0.43 %.
From the point of view of the elastic analysis methods, it is observed that :

- the efficiency diagram (1987 issue), the Bree diagram and the lower bound shakedown method are not applicable,
- the upper bound shakedown method appears to be conservative as it forecasts thermal ratchetting,
- the "Japanese method" predicts a stabilization of the deformations at around 1.90 % without, however, taking the creep effects into account. This prediction could, perhaps, be improved by evaluating a specific coefficient, h for the material used,
- the proposal to extend the efficiency diagram method seems to be interesting. Indeed, by including the creep effect, it predicts a final deformation of about 1 %.

The development and validation of these different methods on the basis of experimental results must be continued in order to obtain methods offering a reasonable degree of consevatism.

6 REFERENCES

[1] BELL R.T. (1982) Ratchetting experiments on thin cylinders subject to axially moving temperature front. UKEA Report ND-R-835(R)

[2] CARTER K.F. PONTER A.R.S. LOVE J.B. Simplified rules for the preventing of ratchetting in axisymmetric shells. SMIRT 11 - TOKYO JAPAN 1991 - Paper E07/3

[3] IGARI T. UETA - M. ICHIMIYA - M. KIMURA - K. SATOH - Y. TAKE K.
Advanced evaluation of thermal ratchetting of FBR components. SMIRT 11- TOKYO JAPAN 1991 Paper E08/1

[4] KAGUCHI M. UETA - M. ICHIMIYA - M. KIMURA - K. FUKUDA - Y. SUZUKI M.
Proposal of a new estimation method of thermal ratchetting of cylinders submitted to moving temperature distributions. SMIRT 11 - TOKYO JAPAN 1991 - Paper L04/1

[5] ROCHE R. Practical procedure for stress classification, 2nd International Seminar on Design Codes and Structural Mechanics - LAUSANNE August 1987

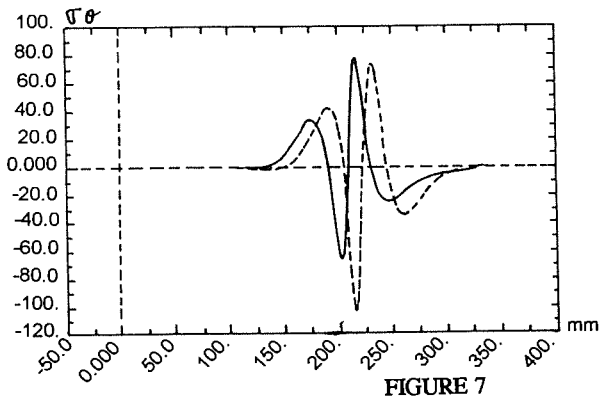

FIGURE 7

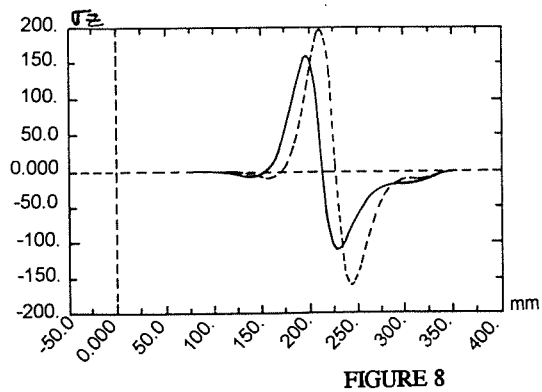

FIGURE 8

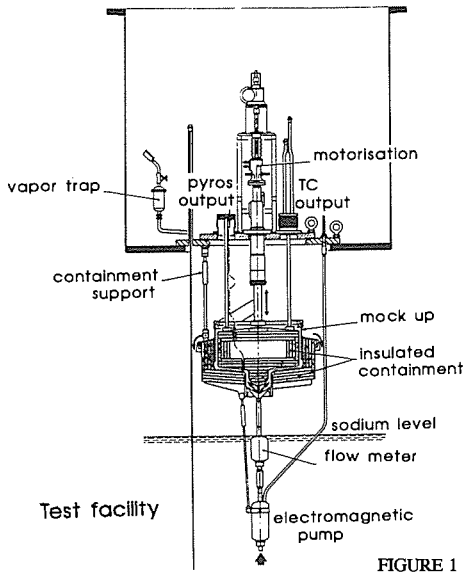

FIGURE 1

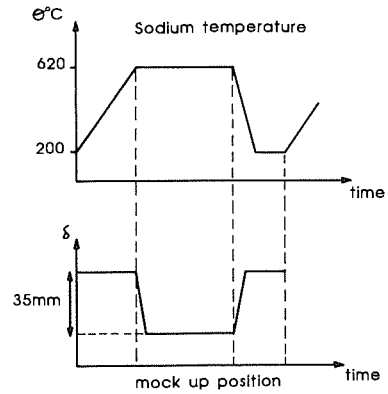

FIGURE 2

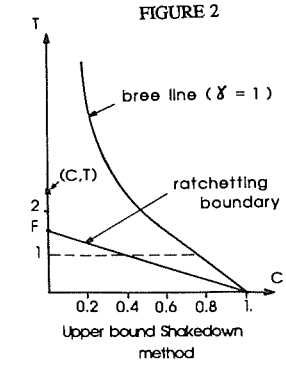

FIGURE 9

LONG SHELL AFTER 500 CYCLES

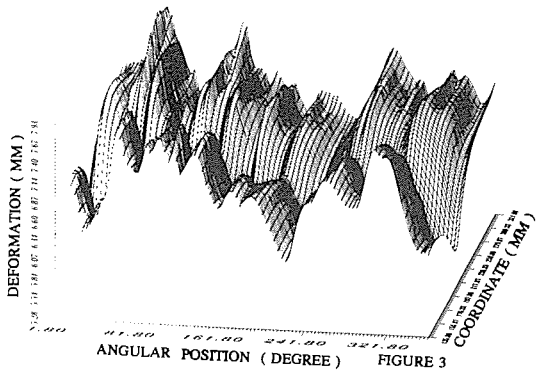

FIGURE 3

LONG SHELL AFTER 500 CYCLES

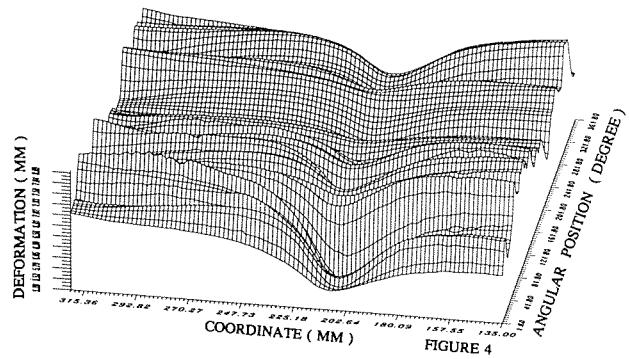

FIGURE 4

LONG SHELL AFTER 700 CYCLES

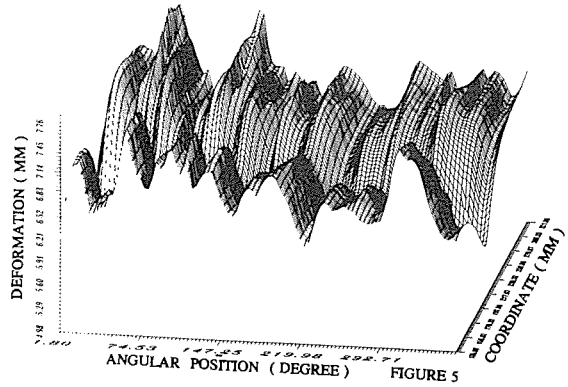

FIGURE 5

SHORT SHELL AFTER 12 CYCLES

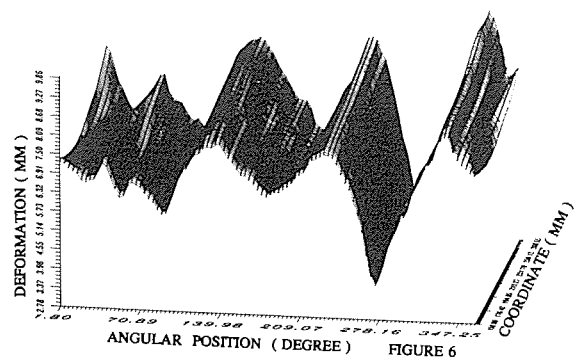

FIGURE 6